Metabolism of apoB-100 in lipoproteins separated by density gradient ultracentrifugation in normal and Watanabe heritable hyperlipidemic rabbits

David M. Shames, Nobuhiro Yamada, and Richard J. Havel

Cardiovascular Research Institute and the Department of Medicine, University of California, San Francisco, CA 94143-1030

Abstract We have examined the capability of a previously developed compartmental model to explain the kinetics of radioiodinated apolipoprotein (apo) B-100 in very low density lipoproteins (VLDL), intermediate density lipoproteins (IDL), and low density lipoproteins (LDL) separated by density gradient ultracentrifugation after intravenous injection of radioiodinated VLDL into New Zealand white (NZW) and Watanabe heritable hyperlipidemic (WHHL) rabbits. Our model was developed primarily from kinetics in whole blood plasma of apoB-100 in particles with and without apoE after intravenous injection of large VLDL, total VLDL, IDL, and LDL. When the initial conditions for this model were assumed to be an intravenous injection of radiolabeled VLDL, the plasma VLDL and LDL simulations for NZW rabbits and the VLDL, IDL, and LDL simulations for WHHL rabbits were found to be inconsistent with the observed density gradient data. By adding a new pathway in the VLDL portion of the model for NZW rabbits and a new compartment in VLDL for WHHL rabbits, and by assuming some cross-contamination in the density gradient ultracentrifugal separations, it was possible to bring our model, which was based upon measurements of ^{125}I-labeled apoB-100 in whole plasma, into conformity with the data obtained by density gradient ultracentrifugation. The relatively modest changes required in the model to fit the gradient ultracentrifugation data support the suitability of our approach to the kinetic analysis of the metabolism of apoB-100 in VLDL and its conversion to IDL and LDL based upon measurements of ^{125}I-labeled apoB-100 in whole plasma after injection of radiolabeled VLDL, IDL, and LDL. Furthermore, the differences in kinetics observed by us between data from whole plasma and data from plasma submitted to ultracentrifugal separation from the same or similar animals highlight the fact that small variations that can occur in the separation of lipoprotein classes by buoyant density can lead to confusing results.—**Shames, D. M., N. Yamada, and R. J. Havel.** Metabolism of apoB-100 in lipoproteins separated by density gradient ultracentrifugation in normal and Watanabe heritable hyperlipidemic rabbits. *J. Lipid Res.* 1990. **31:** 753–762.

Supplementary key words VLDL • LDL • kinetic analysis • fractional turnover rate • multicompartmental model

In humans, low density lipoproteins (LDL) were originally observed as a distinct species by analytical ultracentrifugation (1) and were largely separated from a species of slightly higher flotation rate, now called intermediate density lipoproteins (IDL). In rabbits, IDL and LDL form an ultracentrifugal continuum (2–4), resembling more that of certain abnormal humans, particularly those with familial dysbetalipoproteinemia (5). In order to examine systematically the kinetics of apoB-100 in normal (New Zealand white, NZW) and Watanabe heritable hyperlipidemic (WHHL) rabbits and to define the kinetic behavior of species of VLDL, IDL, and LDL that contain apoE (B,E particles) or lack this protein (B particles) (6–8), we developed a method for analysis of radioiodinated apolipoprotein (apo) B-100 in whole plasma after the injection of very low density lipoproteins (VLDL), IDL, and LDL separated by sequential ultracentrifugation and purified by recentrifugation (9). With this method, ultracentrifugal separation of lipoprotein fractions was limited to the injectates.

In some of these experiments, we separated lipoproteins from the plasma by density gradient ultracentrifugation in order to test our whole blood plasma-based model of apoB-100 kinetics. We anticipated that separation of multiple fractions in swing-out rotors would allow us to examine productively the process of conversion of apoB-100 to particles of progressively increasing density, despite the lack of clear definition of IDL from LDL. In particular, we postulated that samples separated in this way would be subject to less cross-contamination than might be observed with the use of angle head rotors and that the results of kinetic analysis based on these data would be consistent with those obtained in the same animals by analysis of radioiodinated apoB-100 in whole blood plasma. The results of this examination are described here.

Abbreviations: VLDL, very low density lipoproteins; IDL, intermediate density lipoproteins; LDL, low density lipoproteins; NZW, New Zealand white; WHHL, Watanabe heritable hyperlipidemic.

MATERIALS AND METHODS

Preparation of lipoprotein fractions

The normal and WHHL rabbits in which the experiments reported here were carried out were those used in the reported studies of apoB-100 radioactivity in whole plasma after injection of radioiodinated VLDL ($d < 1.006$ g/ml) (6, 7). Density gradients were constructed as described previously for samples of liver perfusates (7) by layering 2.0 ml of water and 2.1 ml 0.64 M NaCl (1.025 g/ml) above 0.5 ml plasma diluted to a volume of 2.1 ml NaCl at a final nonprotein solvent density of 1.050 g/ml in a 1.3 × 6.4 cm diameter centrifuge tube. The tubes were centrifuged in a SW 41 rotor in a Beckman preparative ultracentrifuge (Beckman Instruments, Palo Alto, CA) at 39,000 rpm for 22 h at 12°C. The top fraction was obtained by tube slicing and the tube wall was rinsed with 0.5 ml water. Then 11 fractions of 0.5 ml were obtained sequentially by careful aspiration at the meniscus (7). The density of each fraction was measured with a conductivity meter, and radioiodinated apoB was measured as described (9). Mean recovery of whole plasma ^{125}I-labeled apoB in the summed fractions was 93.3 ± 4.1% (SD) for NZW rabbits and 96.2 ± 3.7% for WHHL rabbits.

Of the 11 fractions obtained in these studies, only the first 8 contained appreciable radioiodinated apoB. For the series of experiments in five NZW rabbits, fractions 1 and 2 contained lipoproteins with the density of VLDL; fractions 3–5, lipoproteins with the density of IDL; and fractions 6–8, lipoproteins with the density of LDL. For the series of experiments in six WHHL rabbits, performed at a later time, the same separations were obtained except that VLDL were confined to fraction 1 and IDL included fractions 2–5 (**Table 1**).

Kinetic analysis

A compartmental model has been developed by us describing the kinetics in whole plasma of apoB-100 in B,E and B particles in large VLDL, small VLDL, IDL, and LDL for both NZW and WHHL rabbits (6–8). This model is based on apoB-100 tracer data in whole plasma (not subjected to ultracentrifugation) after intravenous injection of radiolabeled LDL, IDL, total VLDL, and large VLDL into NZW and WHHL rabbits. The data were further refined by analyzing the distributions of apoB-100 in B,E and B particles separated by anti-apoE immunoaffinity chromatography. Data on the accumulation of apoB-100 in perfusates of isolated livers from NZW and WHHL rabbits were also used in the development of this model (10).

Briefly, this analysis took the form of developing a compartmental model for B,E and B particles in LDL after injection of LDL. Similar analyses were performed for IDL and VLDL by assuming that the LDL portion of the model is known for analysis of whole plasma data after injection of IDL and that the LDL and IDL portions of the model are known for analysis of whole plasma data after injection of VLDL. Eventually, all parameters of the model were adjusted to all three sets of whole plasma data at the same time to obtain the best estimates of the parameter values. Finally, the VLDL portion of the model was expanded to accommodate B,E and B particle data in whole plasma following injection of large VLDL.

The current analysis is an investigation into how well our model explains the concentration of apoB-100 radioactivity in lipoprotein fractions separated by density gradient ultracentrifugation and summed over the density ranges corresponding to VLDL, IDL, and LDL in these rabbits after injection of total VLDL. These data were ob-

TABLE 1. Densities of lipoprotein fractions from density gradients

Fraction		NZW (n = 5)	WHHL (n = 6)	
		g/ml		
1	VLDL	1.0022 (0.00015)[a]	1.0052 (0.00039)	VLDL
2	VLDL	1.0046 (0.00094)	1.0074 (0.00037)	
3	IDL	1.0082 (0.00052)	1.0106 (0.00054)	IDL
4	IDL	1.0115 (0.00062)	1.0135 (0.00044)	IDL
5	IDL	1.0182 (0.00052)	1.0184 (0.00060)	IDL
6	LDL	1.0224 (0.00099)	1.0227 (0.00114)	
7	LDL	1.0283 (0.00070)	1.0278 (0.00127)	LDL
8	LDL	1.0340 (0.00095)	1.0329 (0.00130)	LDL

[a]Mean values and SD (in parentheses).

tained concurrently with the data on radioiodinated apoB in B,E and B particles in whole plasma in the same animals for the WHHL rabbits and in a matched set of NZW rabbits.

We define the "response of a model" to a stimulus as the simulation generated from the model to a given set of initial conditions (11). The responses for apoB-100 in VLDL, IDL, and LDL were generated assuming initial conditions for VLDL injection as the stimulus. These initial conditions (Table 3 in reference 8) were obtained from the combined analysis of the data for B,E and B particles in whole plasma after large and total radiolabeled VLDL were injected into NZW and WHHL rabbits. The response for apoB-100 in plasma VLDL was obtained by summing the individual compartmental responses for "fast" and "slow" B,E and B particles in the VLDL portion of the model. The responses for apoB-100 in plasma IDL and LDL were obtained by summing the B,E and B responses in IDL and LDL particles, respectively, for both NZW and WHHL rabbits.

The concentrations of ^{125}I-labeled apoB-100 radioactivity in the density gradient fractions were summed for the density ranges corresponding to VLDL, IDL, and LDL, respectively, and compared with the model-generated responses. Even cursory inspection of the simulated responses (**Fig. 1, A and B,** solid curves) for VLDL, IDL, and LDL revealed poor fits to the density gradient data points in both NZW and WHHL rabbits. In NZW rabbits, the apoB-100 model-generated response for VLDL fell more slowly than that observed with VLDL separated by density gradient ultracentrifugation at times beyond 1 h after injection (Fig. 1A). To fit the later time points for apoB-100 in VLDL, the fractional turnover rate of slow B particles in our model had to be increased. We elected to effect this change by introducing an additional pathway: the conversion of slow B particles in VLDL to slow B,E particles. To remain consistent with the immunoaffinity data in whole plasma, the fractional rate of irreversible loss from the plasma of slow B,E particles in VLDL also had to be adjusted upward to compensate for the in-

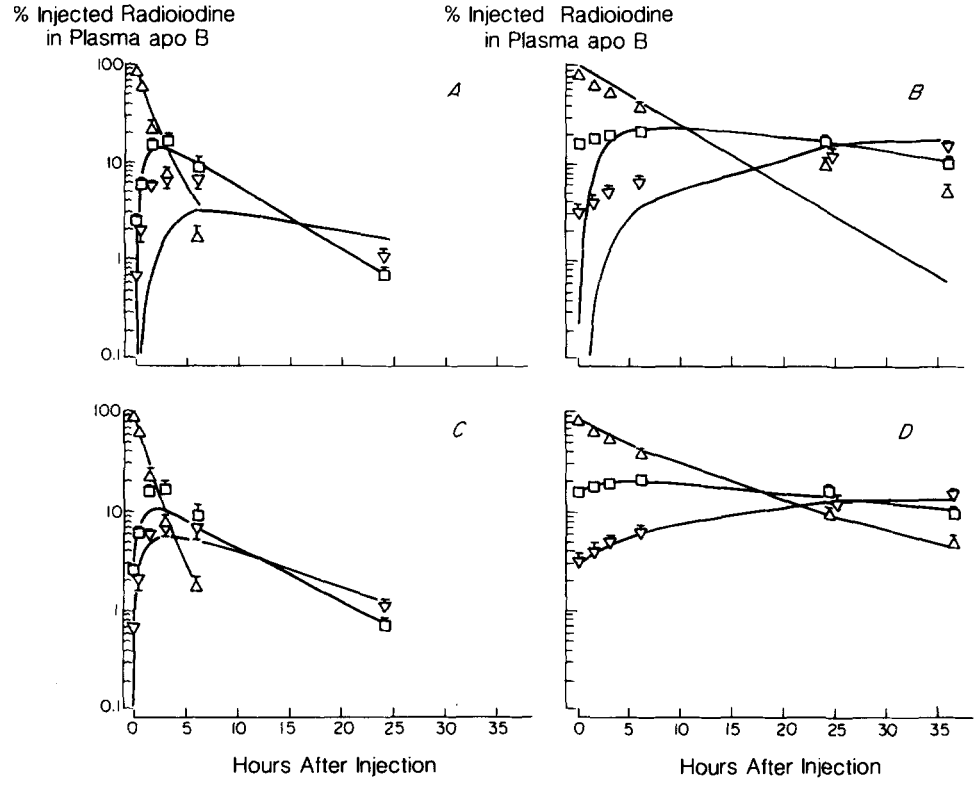

Fig. 1. Mean values for the percent of labeled apoB-100 in VLDL (△), IDL (□), and LDL (▽) in NZW (panels A and C) and WHHL rabbits (panels B and D) after injection of radioiodinated VLDL. Bars represent 1 SE (where not shown, SE values fall within data points). The results are expressed as % of the initial value, which was estimated by dividing the counts per min of the injected ^{125}I-labeled apoB-100 by the plasma volume, taken as 45 ml/kg body weight. Panels A and B show responses (solid curves) generated from model, previously developed by us, based on whole plasma data from NZW and WHHL rabbits. These responses are compared with density gradient data summed over the fractions corresponding to VLDL, IDL, and LDL density ranges. Panels C and D show the best fits obtained to the density gradient data by combinations of the expanded model responses for VLDL, IDL, and LDL assuming cross-contamination in the density gradient data (see text).

creased radioactivity coming into the slow B,E compartment from the slow B compartment. Although the model-generated response for IDL fit the data well, that for LDL yielded a much slower increase in radioiodinated apoB-100 than that observed with the density gradient data. In terms of our model, this suggested that the relatively rapid rise of the radioactivity of apoB-100 in LDL separated by density gradient ultracentrifugation could be the result of contamination of LDL by IDL.

Inspection of the responses generated from the model for VLDL, IDL, and LDL in WHHL rabbits (Fig. 1B, solid curves) revealed poor fits to the density gradient data points for all three lipoprotein fractions, even during the first few minutes after injection. In the sample taken 3 min after injection, 80.0% of the injected ^{125}I-labeled apoB-100 was in VLDL, 15.5% in IDL, and 3.0% in LDL (mean values for the six experiments). These values are close to those observed when samples of the injected VLDL were mixed with the recipient's plasma taken before injection, incubated on ice for 30 min, and then subjected to density gradient ultracentrifugation. (The amount of labeled VLDL added to the plasma was comparable to that obtained by mixing the injected VLDL with blood plasma in vivo). These mixing experiments, performed in five of the six experiments with WHHL rabbits, gave mean values of 83.2% of ^{125}I-labeled apoB-100 in VLDL, 14.4% in IDL, and 2.4% in LDL. Thus, there was little or no conversion of the radioiodinated apoB-100 injected into lipoproteins of higher density during the first 3 min. Since much less of the injected VLDL appeared in lipoproteins of higher density 3 min after injection into NZW rabbits, an appreciably larger fraction of the injected VLDL from WHHL rabbits presumably had a density close to the limiting value of 1.006 g/ml used to distinguish VLDL from IDL.

In WHHL rabbits, the VLDL response from the model (Fig. 1B, solid curve) suggested levels of ^{125}I-labeled apoB-100 that were noticeably higher than those observed in VLDL separated by density gradient ultracentrifugation during the first 6 h and much below thereafter. The latter discrepancy is consistent with some contamination of VLDL separated by density gradient ultracentrifugation with particles of higher density and slower turnover (presumably IDL). However, the values for ^{125}I-labeled apoB-100 in the least dense of the IDL fractions (fraction 2 in **Fig. 2**) at 24 and 36 h after injection are much too low for contamination with IDL to be an important cause of the reduced rate of ^{125}I-labeled apoB-100 clearance in VLDL at these late times. It is thus evident that apoB-100 in VLDL of WHHL rabbits has a slowly turning-over fraction with kinetic properties similar to IDL, which produces the slow plasma clearance at 24 and 36 h. This fraction was not detected in the kinetic analysis of whole plasma data from these rabbits (7, 8). Consequently, a new VLDL compartment of B,E particles having IDL kinetics has been added to the VLDL portion of our model for WHHL rabbits.

Finally, both the IDL and LDL responses of the WHHL model rose much too slowly to explain the observed levels of ^{125}I-labeled apoB-100 in IDL and LDL separated by density gradient ultracentrifugation. This result is consistent with appreciable contamination of

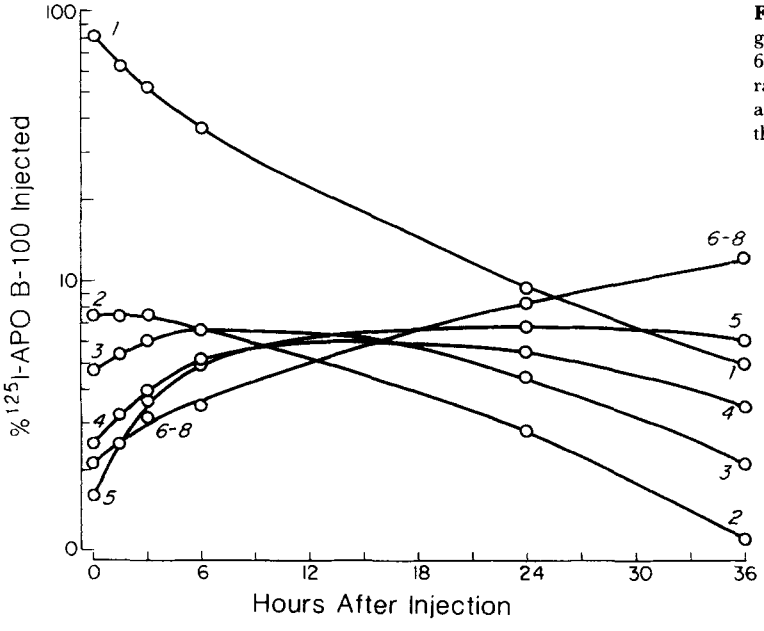

Fig. 2. Mean values for the percent of labeled apoB in density gradient fractions 1 through 5 and combined values for fractions 6 through 8 after injection of radioiodinated VLDL into WHHL rabbits. Fraction 1 corresponds to VLDL, fractions 2-5 to IDL, and fractions 6-8 to LDL (see Table 1). Lines are drawn smoothly through the points for each fraction.

IDL with particles having VLDL kinetics and at least some contamination of LDL with particles having IDL kinetics.

To test the hypothesis that combinations of the VLDL, IDL, and LDL responses generated from our model could explain the density gradient data for VLDL, IDL, and LDL, various linear combinations of these model responses were formulated with the aid of the SAAM and CONSAM computer programs (12, 13) (Appendix). The optimal set of linear combinations of model responses was calculated from the best fit to all the density gradient data from NZW and WHHL rabbits. Nonlinear parameter adjustments allowed in the model were: *1*) in the NZW model, two fractional turnover rates (one new) for VLDL needed as described above to explain the more rapid kinetics of VLDL separated by density gradient ultracentrifugation in these animals; and *2*) in the WHHL model, the fractional rate of irreversible loss from the plasma of B,E particles in VLDL from a compartment with intermediate kinetics and the fractional conversion of particles from this compartment to IDL. The two parameters describing the slowest turning-over compartment of B,E particles in VLDL in the WHHL model cannot be determined uniquely from the density gradient data for VLDL and are therefore fixed with values close to those calculated for B,E particles in IDL. The inability to determine uniquely the values for these two parameters is due to the sparsity of our data defining the final slope of the density gradient data for VLDL in the WHHL rabbits.

Concurrently with this fitting procedure, the four adjustable parameters mentioned above were also fitted to all of the data for B,E and B particles in whole plasma to assure that the fits to these data, previously reported by us (8), did not change. All other parameters of the model remained fixed as published (8). The uncertainties for the calculated values of the four fractional turnover rates and the multiple linear parameters were estimated from the covariance matrix at the least squares fit.

RESULTS

Our analysis shows that various linear combinations of the VLDL, IDL, and LDL responses of our expanded model can explain the results obtained by density gradient ultracentrifugation after VLDL injection for both NZW and WHHL rabbits (Fig. 1, C and D). The percentages of the VLDL, IDL, and LDL simulations from our model required to fit the density gradient data are shown in **Table 2.** In NZW rabbits, the VLDL density gradient data could be fitted by the VLDL time activity curve generated from the model. The best fit to the IDL density gradient data in NZW rabbits required 2% of the VLDL response, 70% percent of the IDL response, and 23% of the LDL response. The LDL density gradient data required 30% of the IDL response of the model and 77% of the LDL response.

In WHHL rabbits the VLDL responses of our model, slightly modified in the B,E portion of VLDL, fitted the VLDL density gradient data well and required 85% of this response. The remaining 15% was required to fit the early time points of the IDL and LDL density gradient data. The IDL data required 12% of the VLDL response of the model, 88% of the IDL response, and 12% of the LDL response. Finally, the LDL density gradient data required 3% of the VLDL response of the model, 12% of the IDL response, and 88% of the LDL response. The average fractional standard deviation of these linear coefficients is 0.08 with a range of 0.004–0.29.

The calculated value in NZW rabbits for the fractional rate of conversion of slow B particles to slow B,E particles in VLDL is 0.154 h^{-1} with a fractional standard deviation of 0.13. The calculated value for the fractional rate of irreversible loss from plasma of slow B,E particles in VLDL is 0.838 h^{-1} with a fractional standard deviation of 0.05. This value is about 18% higher than that calculated when no attempt was made to fit the density gradient data together with the whole plasma immunoaffinity data (8).

TABLE 2. Percentages of model responses required to fit kinetic data for apoB-100 in density gradient fractions obtained after injection of radioiodinated VLDL

Fractions Obtained from Density Gradient[a]	Required Model Responses (%)					
	NZW			WHHL		
	VLDL	IDL	LDL	VLDL	IDL	LDL
VLDL	98			85		
IDL	2	70	23	12	88	12
LDL		30	77	3	12	88

[a]For NZW rabbits, VLDL are fractions 1–2, IDL are fractions 3–5, and LDL are fractions 6–8; for WHHL rabbits, VLDL are fraction 1, IDL are fractions 2–5, and LDL are fractions 6–8 (see Table 1).

No significant changes occurred in the fits of the model to the whole plasma data as presented earlier (8). However, the steady state solution in the NZW model is slightly different because of the increases in the fractional turnover rates of slow B and slow B,E particles in VLDL. The total apoB-100 production rate is now calculated to be 10.28 mg · dl^{-1}h^{-1} as compared with 9.53 mg · dl^{-1}h^{-1}, an 8% increase. This model is shown in **Fig. 3.**

In the WHHL rabbit our model (**Fig. 4**) also reveals some changes from that originally published (8). A single, relatively slowly turning-over compartment of B,E particles in VLDL has been replaced by two compartments with kinetics somewhat faster and somewhat slower than those of the slow compartment of our previous model. The fractional rates of irreversible loss from plasma and conversion to B,E particles in IDL of the more rapidly turning over of these compartments (intermediate B,E particles) are calculated to be 0.144 h^{-1} and 0.101 h^{-1}, respectively. Fractional standard deviations calculated for these two parameters are 0.10 and 0.04, respectively. The fractional turnover rates of irreversible loss from plasma and conversion to IDL for the slowest of the B,E particle compartments in VLDL are not determinable uniquely from the VLDL density gradient data and are fixed at values similar to those of B,E particles in IDL, 0.017 h^{-1} and 0.034 h^{-1}, respectively. As in our previously published model, the fractional rate of conversion of B particles in VLDL to B particles in IDL was assumed to be the same as for B,E particles, in this case that of intermediate B,E particles. The value for this parameter is 0.101 h^{-1}.

No significant changes in the fits of our WHHL model to the whole plasma B,E and B immunoaffinity data (8) occurred. Slight changes occurred in the steady state solution resulting from the addition of a new B,E particle compartment in VLDL. The total apoB-100 production rate increased to 8.87 mg · dl^{-1}h^{-1}, a value 14% greater than that suggested by our previous model. All other changes in transport rates as compared to our previous model were smaller on a percentage basis. The transport rate of slow B,E particles in VLDL to B,E particles in IDL

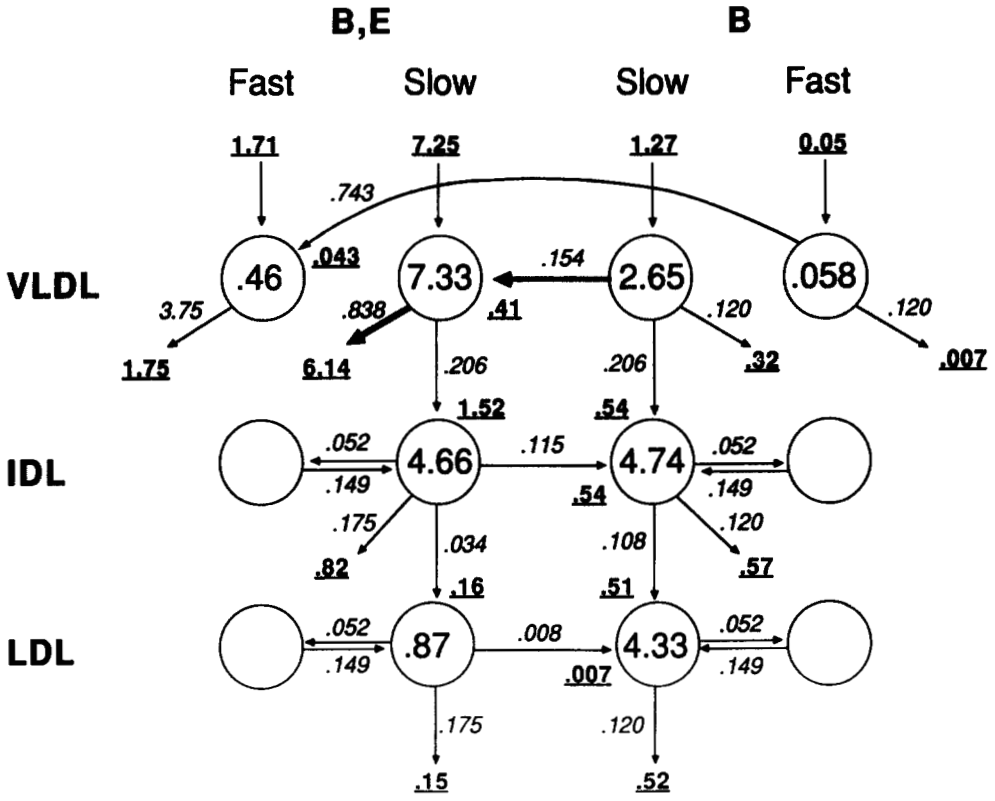

Fig. 3. Multicompartmental model of the metabolism of apoB-100 in NZW rabbits developed from combined analysis of data on radioactivity in apoB-100 in whole plasma (8) and after density gradient ultracentrifugal separation of VLDL, IDL, and LDL (this paper). This model differs from that shown in (8) by addition of a pathway for conversion of slow B particles to slow B,E particles in VLDL. Only two of the rate constants (shown above bold arrows) differ from those obtained from analysis of data in whole plasma alone. The concentrations (mg/dl) of B,E and B particles of lipoprotein classes in the intravascular compartment are shown within the circles. Empty circles represent extravascular compartments for IDL and LDL. Transport rates (mg · dl^{-1}h^{-1}) are underlined. Small, italicized numbers are rate constants (h^{-1}).

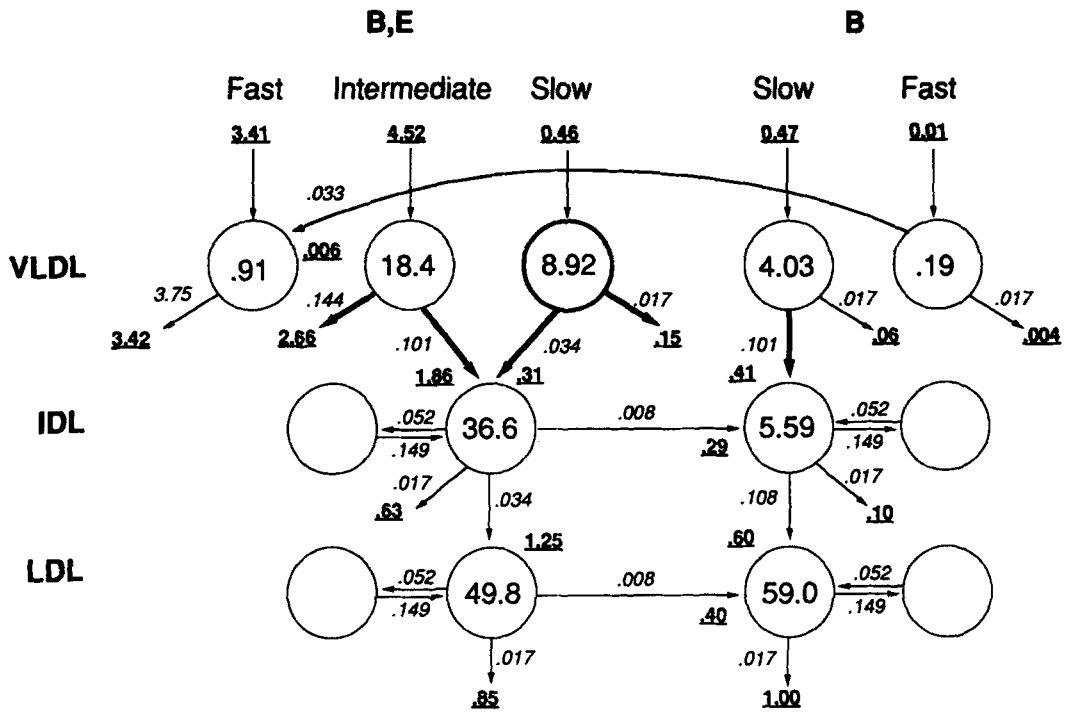

Fig. 4. Multicompartmental model of the metabolism of apoB-100 in WHHL rabbits developed from combined analysis of data on radioactivity in apoB-100 in whole plasma (8) and after density gradient ultracentrifugal separation of VLDL, IDL, and LDL (this paper). This model differs from that shown in (8) by addition of a new B,E particle compartment in VLDL ("slow B,E," heavy line) having IDL B,E kinetics with pathways of irreversible loss and conversion to IDL B,E. The old slow B,E compartment in VLDL has been renamed "intermediate B,E." New values are present for the two new rate constants and three old rate constants (shown next to bold arrows). The concentrations (mg/dl) of B,E and B particles of lipoprotein classes in the intravascular compartment are shown within the circles. Empty circles represent extravascular compartments for IDL and LDL. Transport rates ($mg \cdot dl^{-1}h^{-1}$) are underlined. Small, italicized numbers are rate constants (h^{-1}).

(the new pathway) was 0.31 $mg \cdot dl^{-1}h^{-1}$, a value representing 14% of the B,E transport from VLDL to IDL and 12% of the total apoB-100 transport from VLDL to IDL.

DISCUSSION

We previously formulated a compartmental model that could explain the kinetics of apoB-100 in B,E and B particles in whole plasma of NZW and WHHL rabbits after injection of radioiodinated large VLDL, total VLDL, IDL, and LDL, and was consistent with both the steady state concentration of these lipoproteins and data from isolated hepatic perfusion experiments. We found that this logical structure could not explain the kinetics of apoB-100, separated by density gradient ultracentrifugation after injection of radioiodinated VLDL, in VLDL and LDL of a matched set of NZW rabbits and in VLDL, IDL, and LDL of the same WHHL rabbits.

Our model could be brought into conformity with the density gradient data when small additions were made to the model and when we hypothesized that the density gradient separations of VLDL, IDL, and LDL were imperfect, such that various fractions were somewhat contaminated with adjacent fractions. The greatest cross-contamination appeared to occur between IDL and LDL in NZW rabbits and to a lesser extent in WHHL rabbits. This is not surprising given the ultracentrifugal continuum known to exist between IDL and LDL in the rabbit (2-4). The moderate estimated contamination in WHHL rabbits of the IDL density gradient fractions by VLDL (12%) may be explainable from the fact that the mean density of the lightest IDL fraction in WHHL rabbits (1.0074 g/ml) was somewhat lighter than its counterpart in NZW rabbits (1.0082 g/ml); the latter showed only 2% contamination of IDL with VLDL. Furthermore, any ultracentrifugal procedure will tend to yield cross-contamination between fractions whenever the concentration of lipoproteins is appreciable at the density selected to separate one fraction from another. Consequently, the fact that VLDL in WHHL rabbits are appreciably smaller than VLDL in NZW rabbits (4), and may therefore have a higher relative concentration near the limiting density of 1.006 g/ml, is another possible explanation for greater cross-contamination of IDL with VLDL in the WHHL rabbit.

An alternative explanation for the substantial amount of radioactivity in IDL and LDL from WHHL rabbits soon after VLDL injection is rapid conversion of VLDL

to IDL and LDL. This hypothesis must be rejected here because ultracentrifugal separation of the injectates in density gradients yielded a spectrum of apoB-100 radioactivity in the three lipoprotein classes that did not differ appreciably from that found when blood plasma obtained 3 min after injection was submitted to density gradient ultracentrifugation.

To some extent, the problem of cross-contamination of IDL with VLDL in WHHL rabbits may apply as well to the "purified" radioiodinated VLDL that were injected. The injected VLDL were separated in an angle head rotor, but were recentrifuged under similar conditions, which should have reduced contamination substantially. However, the presence of a small amount of lipoprotein at or slightly exceeding the limiting density of 1.006 g/ml cannot be excluded.

Only modest changes in the VLDL portions of our model were required to explain the density gradient data from both NZW and WHHL rabbits. These were a slight increase in the fractional turnover rates of slow B,E and B particles in the NZW model and the addition of a new slowly turning-over B,E particle compartment in the WHHL model. The latter was required to explain the 24- and 36-h observations for the VLDL separated on a density gradient. Despite these changes in the model, changes in the steady state solution were small. The largest were in the production rates of apoB-100, which increased by 8% in the NZW rabbit and 14% in the WHHL rabbit. Thus, as in our earlier analyses (8), there was little difference between the production rates of apoB-100 in the two groups. On the whole, the detailed information provided by the density gradient data tended to corroborate the kinetic analysis we were able to perform using data on the concentration of ^{125}I-labeled apoB-100 in whole plasma after injection of radiolabeled VLDL, IDL, and LDL. The latter approach limits the use of ultracentrifugation to isolation of the injectates, which can be purified by recentrifugation. It has the advantage of being considerably simpler from an experimental point of view and does tend to overcome problems associated with ultracentrifugal cross-contamination. Although the complexity of the kinetic analysis that must be employed to evaluate whole plasma data is somewhat greater than that sometimes used, this analysis is quite tractable with a computer program such as SAAM. Finally, such a technique may be required when ultracentrifugation distorts a particular analysis, such as the separation of B,E from B particles.

The steady state solutions based on our analyses of the kinetics of apoB-100 in B,E and B particles in whole plasma from both NZW and WHHL rabbits are consistent with data obtained with isolated perfused rabbit livers from these animals. The latter data show that virtually all apoB-100 enters the plasma as lipoprotein particles with a density less than 1.006 g/ml (6, 10). Other studies on the kinetic behavior of apoB-100 in VLDL injected into intact NZW rabbits are inconsistent with these hepatic perfusion data (14). In those studies, the conclusion was drawn from analysis of the kinetics of conversion of radioiodinated VLDL to LDL that a significant portion of LDL are not derived from VLDL but instead enter blood plasma independently. The moderate ultracentrifugal cross-contamination that probably occurred in these experiments with angle-head rotors does not appear to offer an explanation for the difference from conclusions drawn by us with respect to de novo production of LDL.

An alternative model to that shown in Fig. 3 can be formulated and shown to be consistent with the density gradient and immunoaffinity data from NZW rabbits. This model allows the fractional rate of irreversible loss from plasma of slow B particles in VLDL to increase above the value for the fractional rate of irreversible loss from plasma of B particles in LDL. Under these circumstances the pathway of conversion of B particles to B,E particles in VLDL, hypothesized in the model shown in Fig. 3, is not necessary. Also the fractional rate of irreversible loss from plasma of B,E particles in VLDL is not changed from the value previously reported, and the increase in production rate of apoB-100 (8) is less than that calculated for the model shown in Fig. 3 (9.94 $mg \cdot dl^{-1}h^{-1}$ versus 10.28 $mg \cdot dl^{-1}h^{-1}$). This alternative is a simpler model than that presented in Fig 3 in that it requires no new parameters. We prefer the model of Fig. 3, however, because we have no reason to believe that B particles in VLDL would have any greater fractional rate of irreversible loss from plasma than that of B particles in LDL. Nevertheless, the differences between these two models are small. Additional data would be required to distinguish between them.

We initially inserted a slowly turning-over VLDL compartment of B,E particles in the model for WHHL rabbits between the slow B,E compartment and the IDL B,E compartment of our previous model. Although this model did explain the VLDL density gradient data and was attractive from the viewpoint of the delipidation cascade, it was inconsistent with the measured plasma concentrations of B,E and B particles in IDL and was therefore discarded for the "parallel" model presented in Fig. 4.

The results shown here apply to NZW and WHHL rabbits fed standard chow diets. Cross-contamination, as hypothesized here, could be larger or smaller under other conditions of study. The extent to which cross-contamination between lipoprotein fractions confounds data in other species is unclear. Packard and associates (15) have shown that angle head ultracentrifugation can yield impure fractions in human experiments and that such contamination can seriously affect the interpretation of kinetic data. We suggest that cross-contamination of kinetically distinct lipoprotein fractions be considered whenever early radio-

activity is seen in IDL and LDL soon after VLDL injection. The possibility of rapid conversion of VLDL to IDL and LDL as an explanation of this phenomenon can be assessed by mixing the injectate with plasma and submitting the mixture to the same ultracentrifugal separation used for the samples of plasma obtained after injection of the VLDL in vivo.

The problems posed for kinetic analysis of lipoprotein tracer data resulting from cross-contamination of kinetically distinct lipoprotein fractions owing to incomplete ultracentrifugal separation are complex and have not been well investigated. The contamination of VLDL with a more slowly turning-over IDL would produce a spuriously low estimation of the fractional catabolic rate of VLDL. However, the calculation of apoB production rate in VLDL may not be affected, assuming that the measurement of apoB mass is performed on the same sample as that used for measurement of radioactivity and has the same measurement error. On the other hand, the contamination of IDL and LDL with VLDL, if not appreciated, would suggest a very rapid conversion of VLDL to IDL and even directly to LDL. In this case, calculation of the VLDL apoB production rate required to explain such a process could spuriously overestimate the actual production rate of apoB in VLDL, and might even suggest a "phantom" pool of apoB in VLDL turning over so rapidly that its disappearance from VLDL would not be observed in the temporal sequence of plasma samples ordinarily employed in such experiments. The effect on kinetic analysis of contamination of LDL with IDL and vice versa is less obvious. Nevertheless, the effects of such cross-contamination would appear to have little influence on calculations of possible de novo production of LDL. Finally, it is worth remembering that the traditional definitions of lipoprotein classes based on buoyant density are operational only. To the extent that the degree of completeness of ultracentrifugal separations of both injectates and plasma samples varies among experiments in the same or different laboratories, differences in kinetic patterns will be observed, even though the metabolic systems from which these kinetics were obtained may be the same or very similar.

APPENDIX

The VLDL, IDL, and LDL responses generated from our NZW model based on an intravenous injection of VLDL are defined as $V_N(t)$, $I_N(t)$, and $L_N(t)$, respectively. Likewise, the corresponding responses from our WHHL model resulting from VLDL injection are defined as $V_W(t)$, $I_W(t)$, and $L_W(t)$, respectively. These responses are obtained by summing the four plasma compartmental responses for VLDL in the NZW model, the five compartmental responses for VLDL in the WHHL model, and the two plasma compartmental responses each for IDL and LDL in the NZW and WHHL models, respectively. If $V'_N(t)$, $I'_N(t)$, and $L'_N(t)$ are defined as the linear combinations of model responses generated in the NZW model to fit the VLDL, IDL, and LDL density gradient data respectively from the NZW rabbits, then

$$V'_N(t) = a_1V_N(t) + b_1I_N(t) + c_1L_N(t)$$
$$I'_N(t) = a_2V_N(t) + b_2I_N(t) + c_2L_N(t)$$
$$L'_N(t) = a_3V_N(t) + b_3I_N(t) + c_3L_N(t)$$

where a_i, b_i, and c_i are linear coefficients representing percentages of the individual model responses for VLDL, IDL, and LDL, respectively. Conservation of mass requires of these linear coefficients that

$$a_1 + a_2 + a_3 = 100$$
$$b_1 + b_2 + b_3 = 100$$
$$c_1 + c_2 + c_3 = 100.$$

A similar set of relations, $V'_W(t)$, $I'_W(t)$, and $L'_W(t)$, was developed to explain the VLDL, IDL, and LDL density gradient data from the WHHL rabbits.

$$V'_W(t) = a_4V_W(t) + b_4I_W(t) + c_4L_W(t)$$
$$I'_W(t) = a_5V_W(t) + b_5I_W(t) + c_5L_W(t)$$
$$L'_W(t) = a_6V_W(t) + b_6I_W(t) + c_6L_W(t)$$

where again

$$a_4 + a_5 + a_6 = 100$$
$$b_4 + b_5 + b_6 = 100$$
$$c_4 + c_5 + c_6 = 100$$

The SAAM 30 program was used to fit $V'_N(t)$, $I'_N(t)$, and $L'_N(t)$ to the NZW density gradient data and $V'_W(t)$, $I'_W(t)$, and $L'_W(t)$ to the WHHL density gradient data. Several of the linear coefficients were calculated to be near zero and were consequently fixed at zero for the final calculations. These were b_1, c_1, and a_3 for the NZW analysis. Calculations of zero for these three coefficients mean that none of the IDL and LDL responses of the model (b_1 and c_1) were required to explain the VLDL density gradient data and none of the VLDL response (a_3) was required to explain the LDL density gradient data. In the WHHL analysis b_4 and c_4 were assumed to be zero in the modelling process. A zero value for b_4 and c_4 means that none of the IDL or LDL responses of the WHHL model were required to explain the VLDL density gradient data. Given the constraints imposed for conservation of mass, three linear coefficients were adjustable for the NZW analysis and four for the WHHL analysis. The calculated values for the linear coefficients are shown in Table 2, and the fits to the density gradient are shown in Fig. 1, C and D.

This work was supported by a grant from the National Institutes of Health (HL-14237) Arteriosclerosis Specialized Center of Research. Dr. Yamada received support from the Yamanouchi Fund.

Manuscript received 17 February 1989, in revised form 20 September, and in re-revised for 3 January 1990.

REFERENCES

1. Gofman, J., F. Lindgren, and H. Elliott. 1949. Ultracentrifugal studies of lipoproteins of human serum. *J. Biol. Chem.* **179:** 973–979.
2. Pierce, F. T. 1954. The interconversion of serum lipoproteins in vivo. *Metabolism.* **III:** 142–153.
3. Terpstra, A. H. M., C. J. H. Woodward, and F. J. Sanchez-Muniz. 1981. Improved techniques for the separation of serum lipoproteins by density gradient ultracentrifugation: visualization by prestaining and rapid separation of serum lipoproteins from small volumes of serum. *Anal. Biochem.* **111:** 149–157.
4. Havel, R. J., T. Kita, L. Kotite, J. P. Kane, R. L. Hamilton, J. L. Goldstein, and M. S. Brown. 1982. Concentration and composition of lipoproteins in blood plasma of the WHHL rabbit. An animal model of human familial hypercholesterolemia. *Arteriosclerosis.* **2:** 467–474.
5. Havel, R. J., J. L. Goldstein, and M. S. Brown. 1980. Lipoproteins and lipid transport. *In* Metabolic Control and Disease. P. K. Bondy and L. E. Rosenberg, editors. W. B. Saunders, Philadelphia, PA. 393–494.
6. Yamada, N., D. M. Shames, J. B. Stoudemire, and R. J. Havel. 1986. Metabolism of lipoproteins containing apolipoprotein B-100 in blood plasma of rabbits: heterogeneity related to the presence of apolipoprotein E. *Proc. Natl. Acad. Sci. USA.* **83:** 3479–3483.
7. Yamada, N., D. M. Shames, and R. J. Havel. 1987. Effect of LDL receptor deficiency on the metabolism of apoB-100 in blood plasma: kinetic studies in normal and Watanabe heritable hyperlipidemic (WHHL) rabbits. *J. Clin. Invest.* **80:** 507–515.
8. Yamada, N., D. M. Shames, K. Takahashi, and R. J. Havel. 1988. Metabolism of apolipoprotein B-100 in large very low density lipoproteins of blood plasma. Kinetic studies in normal and Watanabe heritable hyperlipidemic rabbits. *J. Clin. Invest.* **82:** 2106–2113.
9. Yamada, N., and R. J. Havel. 1986. Measurement of apolipoprotein B radioactivity in whole blood plasma by precipitation with isopropanol. *J. Lipid Res.* **27:** 910–912.
10. Hornick, C. A., T. Kita, R. L. Hamilton, J. P. Kane, and R. J. Havel. 1983. Secretion of lipoproteins from the liver of normal and Watanabe heritable hyperlipidemic rabbits. *Proc. Natl. Acad. Sci. USA.* **80:** 6096–6100.
11. Berman, M. 1963. The formulation and testing of models. *Ann. NY Acad. Sci.* **108:** 182–194.
12. Berman, M., and M. F. Weiss. 1978. SAAM Manual. DHEW Publication No. (NIH) 78-180, National Institutes of Health, Bethesda, MD.
13. Berman, M., W. F. Beltz, P. C. Greif, R. Grabay, and R. C. Boston. 1983. CONSAM User's Guide. U.S. Department of Health and Human Services, Public Health Service, National Institutes of Health, Bethesda, MD.
14. Ghiselli, G. 1982. Evidence that two synthetic pathways contribute to the apolipoprotein B pool of the low density lipoprotein fraction of rabbit plasma. *Biochim. Biophys. Acta.* **711:** 311–315.
15. Packard, C. J., A. Munro, A. R. Lorimer, A. M. Gotto, and J. Shepherd. 1984. Metabolism of apolipoprotein B in large triglyceride-rich very low density lipoproteins of normal and hypertriglyceridemic subjects. *J. Clin. Invest.* **74:** 2178–2191.